



INFLUENCE OF LOADING RATIO ON QUANTIFIED VISIBLE DAMAGES OF R/C STRUCTURAL MEMBERS

N. Takahashi⁽¹⁾

⁽¹⁾ Associate Professor, Tohoku University, ntaka@archi.tohoku.ac.jp

Abstract

The information such as repair cost and downtime is useful for a decision-making in a performance-based seismic design, but the more intuitive information such as the visible damage propagation is assumed to be useful for a decision-making of building owners in the next-generation performance-based seismic design. Therefore the evaluation methods of visible seismic damage for reinforced concrete (R/C) members have been developed in recent years. One of the developed method estimates the propagation of crack length in a very simple way. It is basically combining the empirical and mechanical models, and the models are originally verified under static service load level in CEB-FIP model code for concrete structure (1978). In this paper, this simple method of estimating the crack propagation under seismic load level with large deformation and under dynamic load is verified.

Firstly, to verify the proposed model estimating the crack propagation in a simple way, three R/C beam specimens (F-60, F-90, and FS-90) proportioned to approximately 1/2 of full scale were tested under monotonic static loading. During the service load level (before rebar yielding), estimated total crack length approximates the observed total crack length in each specimen. After rebar yielding (in seismic load level with large deformation), estimated crack lengths of specimen F-60 and F-90 approximates the experimental results. But estimated crack lengths of specimen FS-90 is underestimated the experimental result. Although there is the tendency of underestimating a shear crack length, some accuracy of the simple estimation method for crack length propagation under the static load with large deformation is shown in this case.

Secondly, to verify the proposed model estimating the crack propagation in a quick and easy way under dynamic load, R/C beam dynamic and static test results are employed. The specimen S-5, S-6, S-7, and S-8 are tested under static load (0.1 mm/sec), and the specimen D-5, D-6, D-7, and D-8 are tested under dynamic load (100 mm/sec). Specimens, which ratio of shear strength to flexural strength are around 1.8~1.9, show the almost same damage propagation under static and dynamic load in experimental results. But specimens, which ratio of shear strength to flexural strength are around 2.5~2.6, show the difference of their damage propagation between static loading and dynamic loading, where the dynamic loading results shows the damage around 30% less than that of the static loading. In the proposed simple method, the strain rate effect on the material strength affects slightly the estimation crack length as with experimental results. But an effect of the ratio of shear strength to flexural strength on the crack length difference between static loading and dynamic loading doesn't follow the tendency of experimental result. It is the future issues how to consider key factors like the ratio of shear strength to flexural strength in the proposed simple method.

Keywords: Reinforced concrete, Crack propagation, Seismic Load, Dynamic Load

1. Introduction

The information such as repair cost and downtime is useful for a decision-making in a performance-based seismic design, but the intuitive information such as the visible damage propagation is more useful for a quick decision-making of building owners in the next-generation performance-based earthquake engineering. The powerful evaluation methods of crack propagation for reinforced concrete (R/C) members have been developed in recent years, such as RBSM [1], X-FEM [2]. These analytical tools are very powerful, but these need more time to analyze and higher skill to operate when the structure or the number of members for analysis is getting larger. Therefore, very simple and easy way to estimating crack propagation is proposed in this research. It is basically combining the empirical and mechanical models, and the models were originally verified under static service load level in CEB-FIP code [3]. In this paper, this simple method of estimating the crack propagation are verified under static load with large deformation and under dynamic load, and the results are discussed.

2. Simple Estimation Method of Crack Propagation

2.1 Definition of crack type

Flexural-shear cracks are modelled as bilinear according to the crack growth angle as shown in Fig. 1. Flexural and flexural-shear cracks are estimated based on a fiber model analysis. Kent & Park model [4], Okamura & Maekawa model [5], and bilinear model are employed to the compressive concrete, the tensile concrete, and the reinforcing bar model, respectively. On the other hand, shear cracks are estimated from a stabilized crack pattern after shear cracking strength, where doesn't consider the propagation of shear crack length. The following paragraphs show the detailed process and the example of crack length estimation.

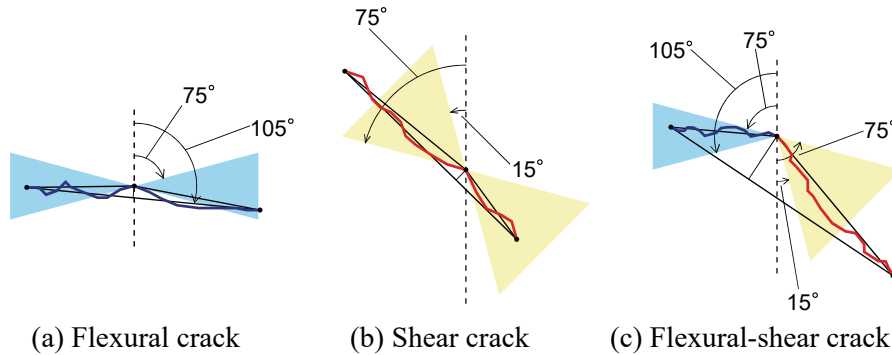


Fig. 1 – Crack type definition due to its angle growth

2.2 Propagation of flexural crack

Flexural cracks generate at the extreme tension fiber where the moment M is larger than flexural cracking moment M_c . This cracking zone, which length is defined as l_{cr} , is expressed as Eq. 1.

$$l_{cr} = \left(1 - \frac{M_c}{M}\right)H \quad (1)$$

where, H : shear span. The number of flexural cracks is also expressed as Eq. 2.

$$n = \frac{l_{cr}}{S_{av}} + 1 \quad (2)$$

where, S_{av} : Average flexural cracking space [6]. The length of flexural crack is defined as the distance from the extreme tension fiber to the point of concrete tensile strength estimated from a fiber model analysis.

2.2 Propagation of flexural-shear crack after the inflection point of flexural crack

To estimate the propagation of flexural-shear cracks after the flexural cracks extending, the inflection points (X_b , Y_b) of flexural-shear cracks are defined shown in Fig. 2. At the inflection point, the angle of principal stress to the axis of the beam calculated from Mohr's stress circle comes under 75 degrees. The crack over the inflection point will propagate to the targets shown in Fig. 3 according to their inflection point coordinates. When an inflection point is included in plastic hinge area, the crack is oriented to the stirrup at critical section in compressive zone. When an inflection point is included without plastic hinge area where is expressed as Eq. 3, the crack is propagate with a constant degrees ϕ to the axis of the beam.

$$Y_{bs} \leq (j_e \cot\phi + S_{m\theta}) - X_{bs} / \tan\phi \quad (3)$$

where, j_e : the distance of stirrup in loading direction, $S_{m\theta}$: average shear cracking space [7], respectively. The length of flexural-shear crack is defined as the sum of the distance from the extreme tension fiber to the inflection point and the distance from the inflection point to the point of converted concrete tensile strength estimated from a fiber model analysis. That is the point where the converted strain ϵ_{bs} , which is assumed to be including the shear strain on discrete crack propagation and expressed as Eq. 4, is larger than the strain of concrete tensile strength ϵ_{cr} .

$$\epsilon_{bs} = \epsilon / \sin\theta \quad (4)$$

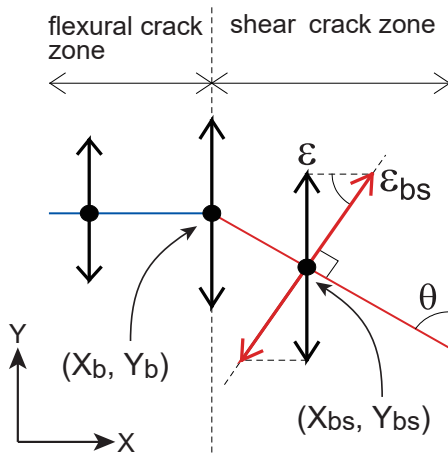


Fig. 2 – Inflection point and converted strain ϵ_{bs}

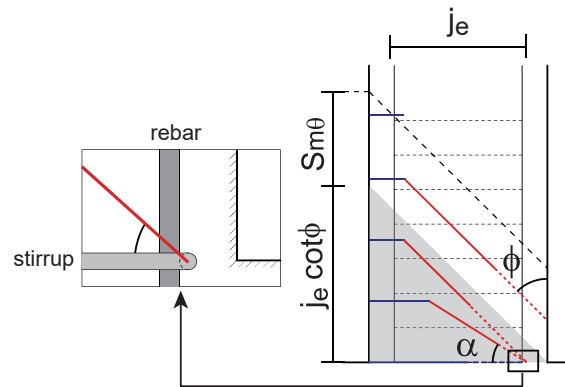


Fig. 3 – Orientation of crack propagation

2.3 Propagation of shear crack

When the shear force is larger than shear cracking strength, shear cracks are generated on the preserved discrete line which excludes the plastic hinge area expressed as Eq. 3. These shear cracks have an average shear crack space $S_{m\theta}$.

3. Verifying the proposed method under static load with large deformation

3.1 Test Specimens, Setup and Instrumentation

Three R/C beam specimens (F-60, F-90, and FS-90) proportioned to approximately 1/2 of full scale were tested under static monotonic loading. The design parameters are given in Table 1. The dimension for the test specimens are shown in Fig. 4, 5 and the test setup are shown in Fig. 6. Crack lengths were measured by CAD tools based on the sketched cracking pattern.

Table 1 – Description of test specimens about monotonic seismic load test [8]

Specimen	Concrete Strength [N/mm ²]	Rebar/ Ratio to the section	Yield strength of rebar [N/mm ²]	Lateral reinforcement/ Ratio to the section	Yield strength of reinforcement [N/mm ²]	Failure mode
F-60	30.5	8-D13 / 0.0067	413 (SD295)	D6@60 / 0.0049	418 (SD295)	Flexure
F-90	32.0			D6@90 / 0.0033	387 (SD345)	Flexure
FS-90	32.5	8-D16 / 0.0104	569 (SD490)	φ9@90 / 0.0066	358 (SR235)	Flexure -Shear

D: diameter of deformed bar φ: diameter of rounded bar

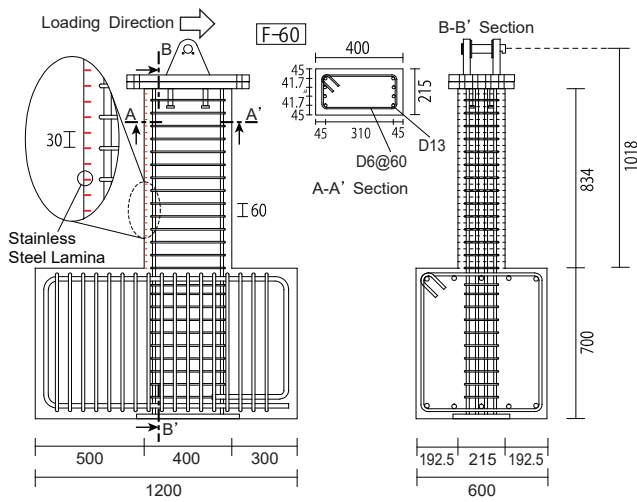


Fig. 4 – Dimension of specimen F-60 [8]

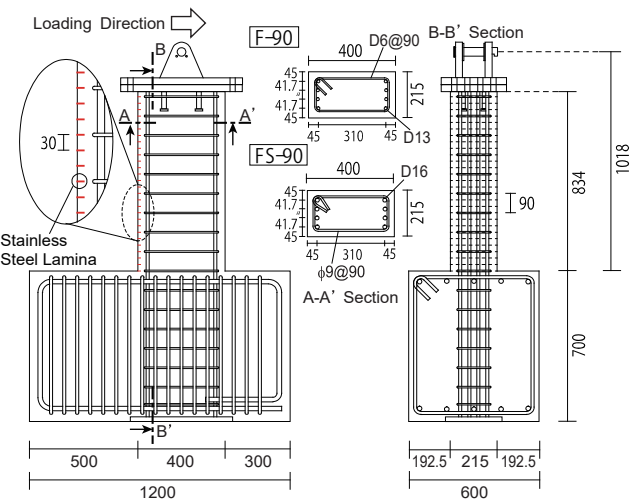


Fig. 5 – Dimension of specimen F-90/FS-90 [8]

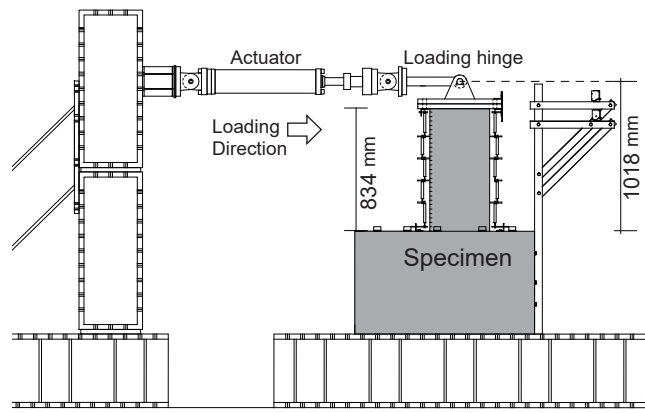


Fig. 6 – Test setup [8]

3.2 Test results

Fig. 7 shows the observed cracking pattern at 0.01[rad.] and Fig. 8 shows the observed crack length versus drift ratio for each specimen, where crack length are divided into crack type shown in Fig. 1. Specimen F-60 and F-90 designed to fail in flexure generated shear cracks after yielding and their shear crack length were the same as their flexural crack length. Specimen FS-90 designed to fail in flexural-shear generated shear cracks after yielding and its shear crack length was twice as long as its flexural crack length. FS-90 specimen has the longest total crack length than F-60 and F-90 specimens.

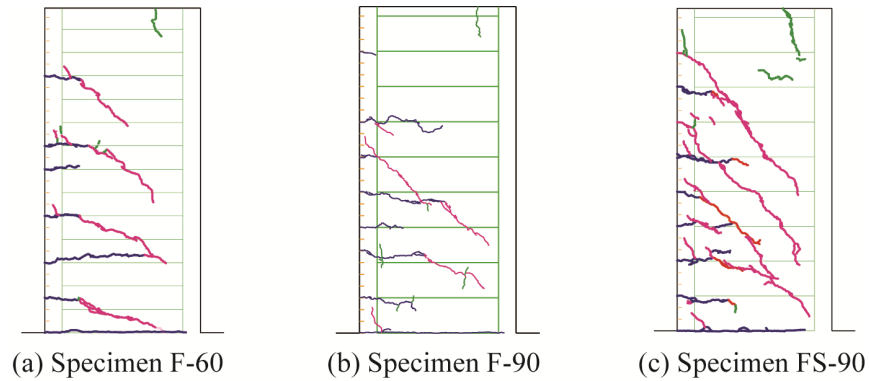


Fig. 7 – Observed cracking pattern (at 0.01[rad.])

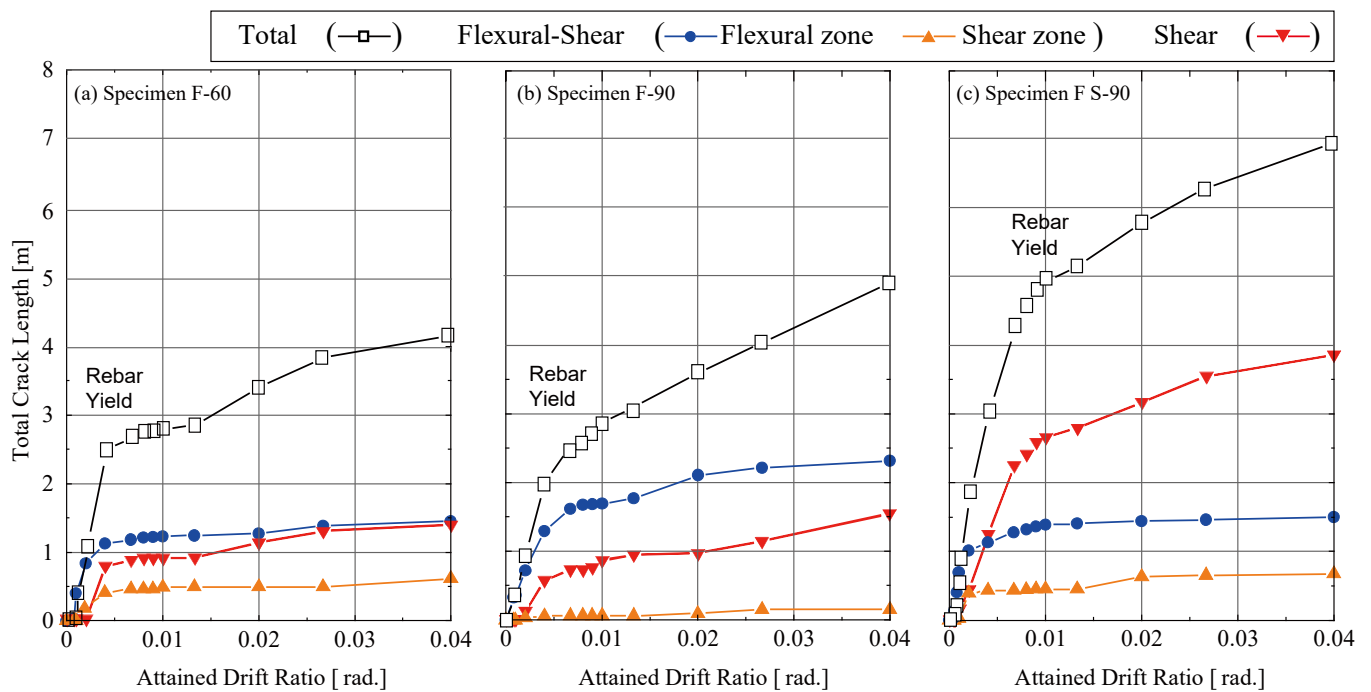


Fig. 8 – Observed crack length

3.3 Estimation results for crack length under static load with large deformation

Fig. 9 shows the estimated cracking pattern at 0.01[rad.] and Fig. 10 shows the comparison of crack length obtained from experimental results and analytical results. During the service load level (before rebar yielding), estimated total crack length approximates the observed total crack length in each specimen. After rebar yielding (in seismic load level with large deformation), estimated crack lengths of specimen F-60 and F-90 approximates or slightly underestimates the experimental results. On the contrary, estimated crack lengths of specimen FS-90 is underestimated the experimental result. The underestimating the crack length of FS-90 might be caused by the failure mechanism which is designed to fail in flexural-shear and provides dominantly shear cracks rather than other specimens (F-60 and F-90). Shear cracks have generally winding path following the coarse aggregate, then the length of shear crack propagation path tends to be larger than the estimated length by the model that consists of straight line.

Although there is the tendency of underestimating a shear crack length, Fig. 10 indicates some accuracy of the simple estimation method for crack length propagation under the static load with large deformation (around 0.01~0.015[rad.]).

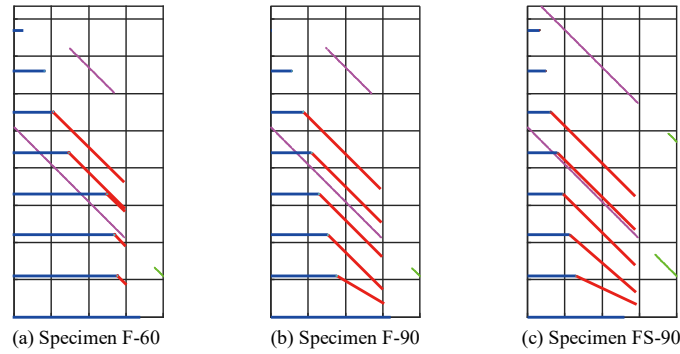


Fig. 9 – Estimated cracking pattern (at 0.01[rad.])

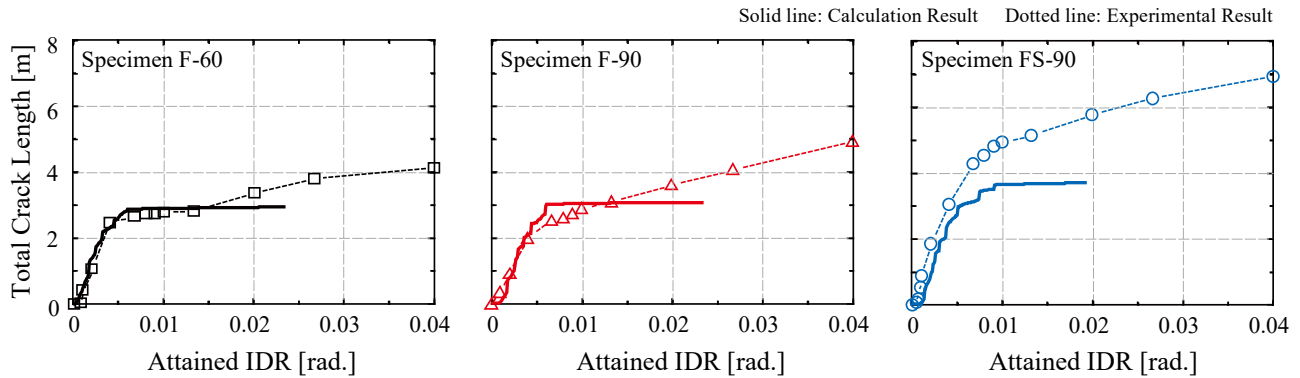
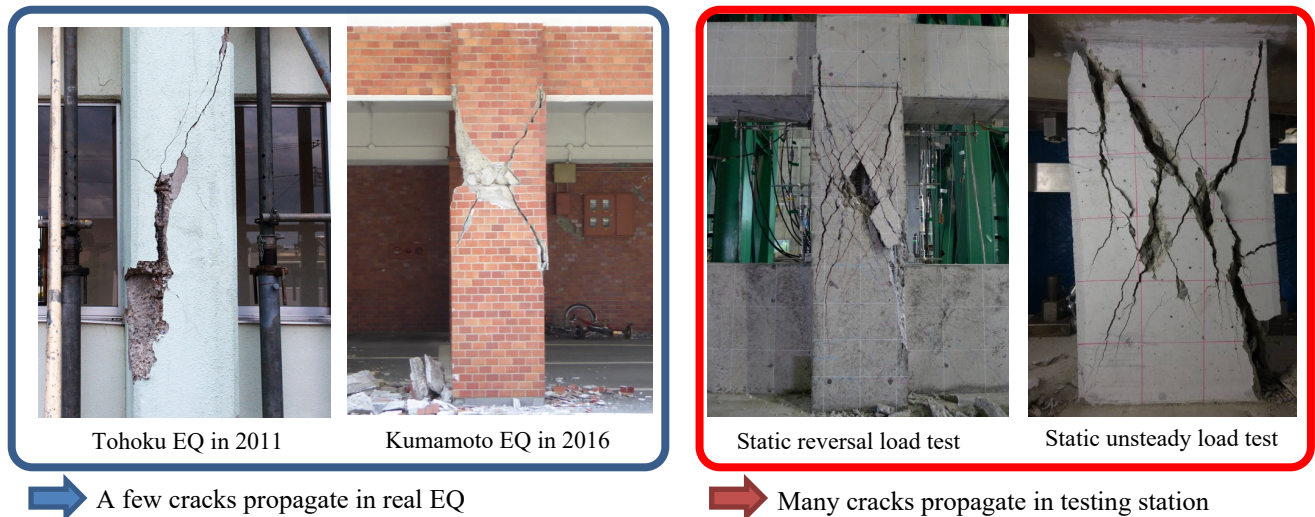


Fig. 10 – Comparison of crack length between the calculation results and experimental results

4. Verifying the proposed method under dynamic load

In the past earthquake reconnaissance, a lot of damage on R/C members were found out. Most of their visible damage seems to be different from the visible damage obtained from many static loading tests. Fig. 11 shows the comparison between the cracking pattern in a real earthquake and in a testing station. In Fig. 11, all of them shows the typical shear failure cracking pattern. Shear crack observed in the earthquake tends to be concentrated, and shear crack observed in the static test tends to be dispersed.

From the material and physical point of view, strain rate effects on the material strength could be relate the above mentioned difference between the cracking pattern under real earthquake (dynamic) load and under static load.



➡ A few cracks propagate in real EQ

➡ Many cracks propagate in testing station

Fig. 11 – Comparison between the crack in real EQ and in testing station

4.1 Test Specimens, Setup and Instrumentation

Eight R/C beam specimens were tested under static and dynamic loading. The design parameters are given in Table 2. The dimension for the test specimens and test setup are shown in Fig. 12 and 13.

Table 2– Description of test specimens about static and dynamic reversal load test [9]

Specimen	Concrete Strength [N/mm ²]	Rebar/ Ratio to the section	Yield strength of rebar/ Yield strength of reinforcement [N/mm ²]	Lateral reinforcement/ Ratio to the section	Average strain rate [x10 ² /sec]	Ratio of Shear Strength to Flexural Strength
S5	27.8	4-D13 + 4-D13 / 0.0085	361(SD345) / 478 (SN400)	2-φ4@80/ 0.0016	-	1.82
D5					3.12	
S6	28.0			2-φ4@40/ 0.0032	-	2.58
D6					3.08	
S7	29.7			2-φ4@80/ 0.0016	-	2.48
D7					2.26	
S8	30.2			2-φ4@40/ 0.0032	-	1.92
D8					3.60	

D: diameter of deformed bar φ: diameter of rounded bar

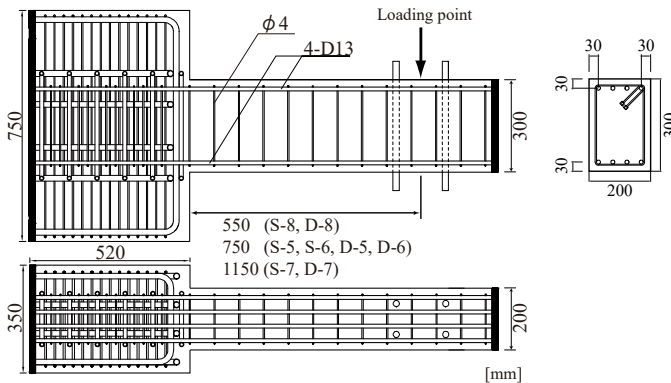


Fig. 12 – Dimension of specimens [9]

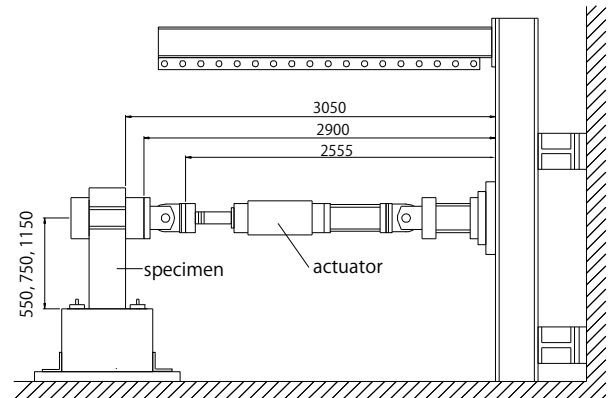




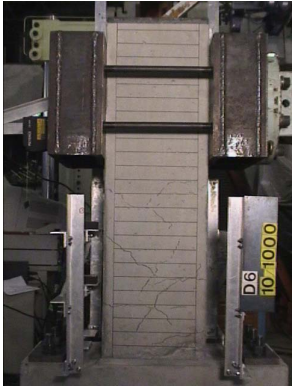
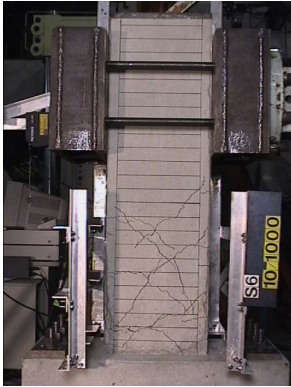
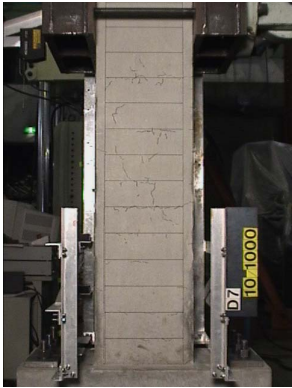
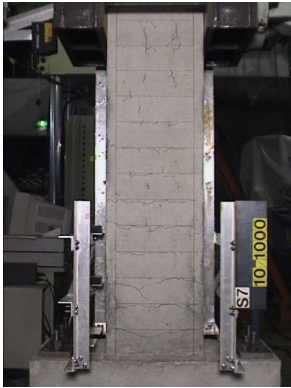
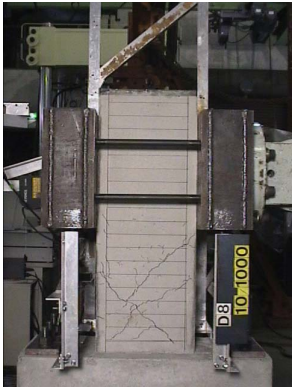
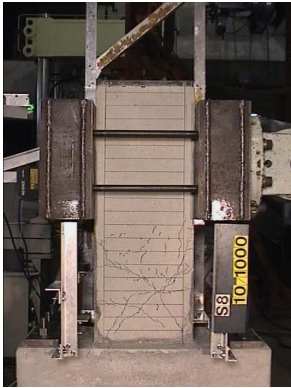
Fig. 13 – Test setup [9]

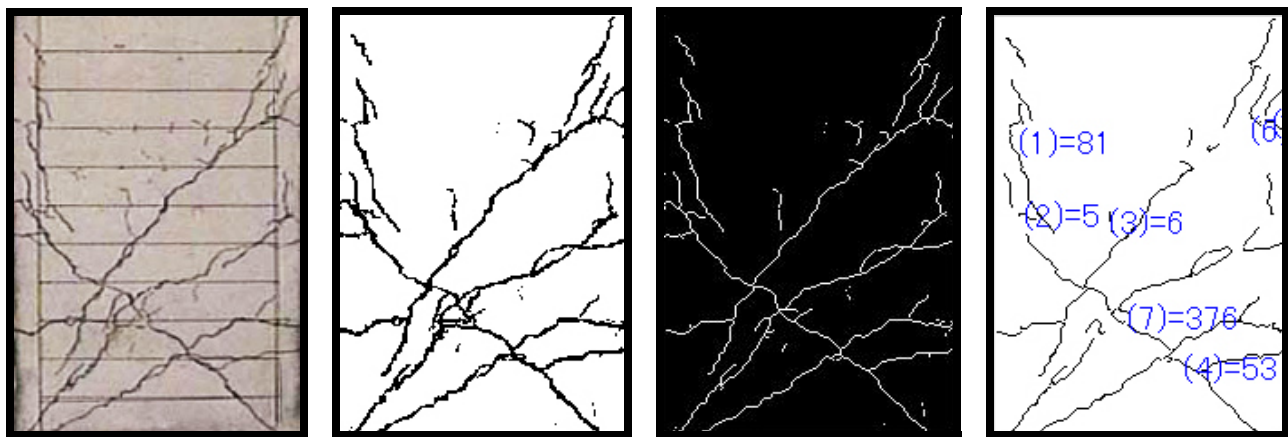
4.2 Test results and damage data acquisition

Table 3 shows the video capture image of each specimen after 7.5/1000 rad. This test series was not prepared for drawing the cracking pattern, and the video during the load was the only data about crack propagation. Therefore, image processing shown in Fig. 14 were employed to get the quantitative damage data. Through the image processing, original captured images are changed to the banalization image, and noise reduction through degenerating the banalization images generate the measurable image about crack length. Table 4 shows the cracking pattern images such as sketch of cracking pattern.

Fig. 15 shows the total crack length of each specimen. In the case of the ratio of shear strength to flexural strength are around 2.5~2.6, Specimens D6 and D7 shows the damage (total crack length) around 30% less than specimens S6 and S7, respectively. On the contrary, in the case of the ratio of shear strength to flexural strength are around 1.8~1.9, specimens D5 and D8 shows the almost same damage (total crack length) as specimens S5 and S8, respectively.

Table 3– Video capture image [9]

	D5	S5	D6	S6
After 7.5/1000 rad. from Video Capture				
	D7	S7	D8	S8
				



(a) Original image (b) Binarization image (c) Noise reduction image (d) Calculate crack length [pixel]

Fig. 14 – Image processing for damage data acquisition

Table 4– Cracking pattern via image processing

	D5	S5	D7	S7
After 7.5/1000 rad. via Image Processing				
	D6	S6		
			D8	S8

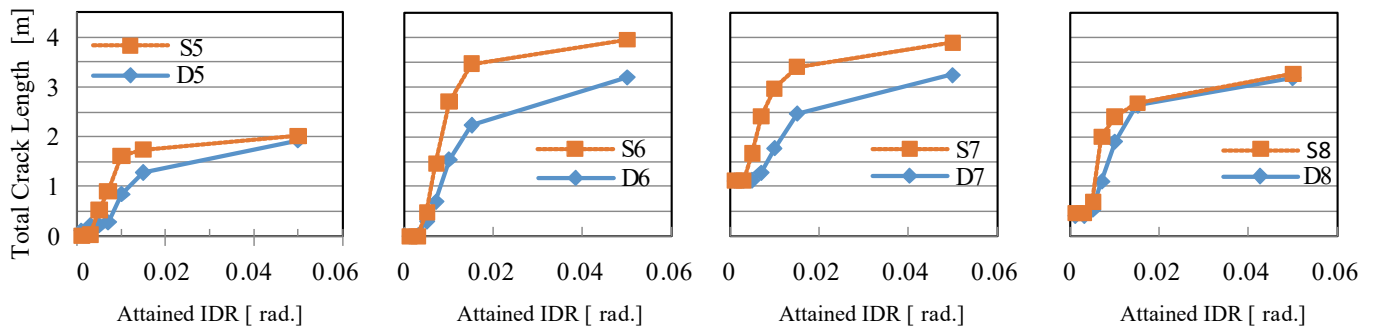


Fig. 15 – Measured total crack length of each specimen

4.3 Estimation results for crack length considering the dynamic load

To consider an effect of dynamic loading, the strain rate effects on the strength was included in the simple method of estimating the crack propagation. Based on the past research[9], Strain rate effects on the steel strength is expressed as Eq. 5.

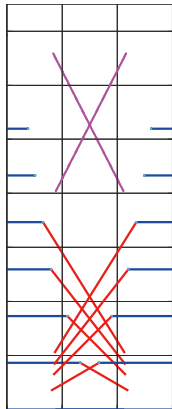
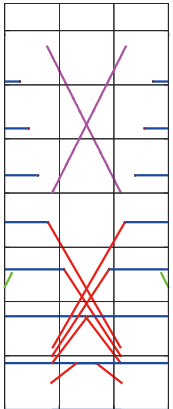
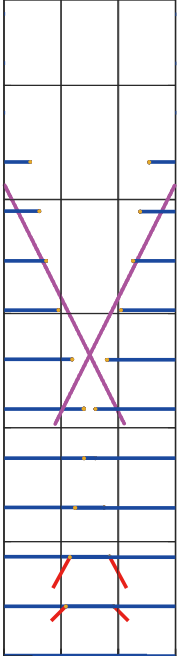
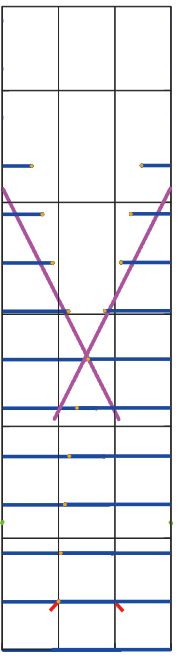
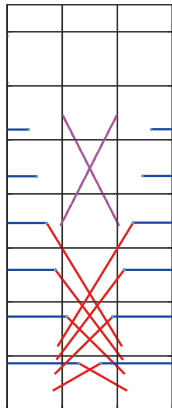
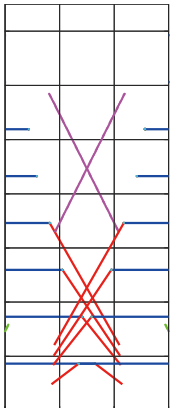
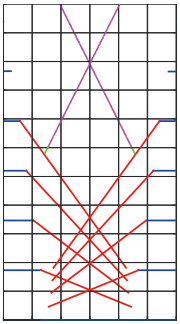
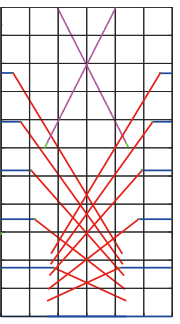
$${}_d f_y = \left(0.9 + 0.05 \cdot \log_{10}(\dot{\epsilon}) \right) \cdot {}_s f_y \quad (5)$$

where, ${}_d f_y$: yield strength of steel under dynamic loading, ${}_s f_y$: yield strength of steel under static loading, and $\dot{\epsilon}$: strain rate [μ /sec]. And strain rate effects on the concrete strength is also expressed as Eq. 6.

$${}_d \sigma_B = \left(0.94 + 0.06 \cdot \log_{10}(\dot{\epsilon}) \right) \cdot {}_s \sigma_B \quad (6)$$

where, ${}_d \sigma_B$: yield strength of concrete under dynamic loading, ${}_s \sigma_B$: yield strength of concrete under static loading, and $\dot{\epsilon}$: strain rate [μ /sec].

Table 5– Estimated cracking pattern

	D5	S5	D7	S7
After 7.5/1000 rad. from estimated crack propagation				
	D6	S6	D8	S8
				

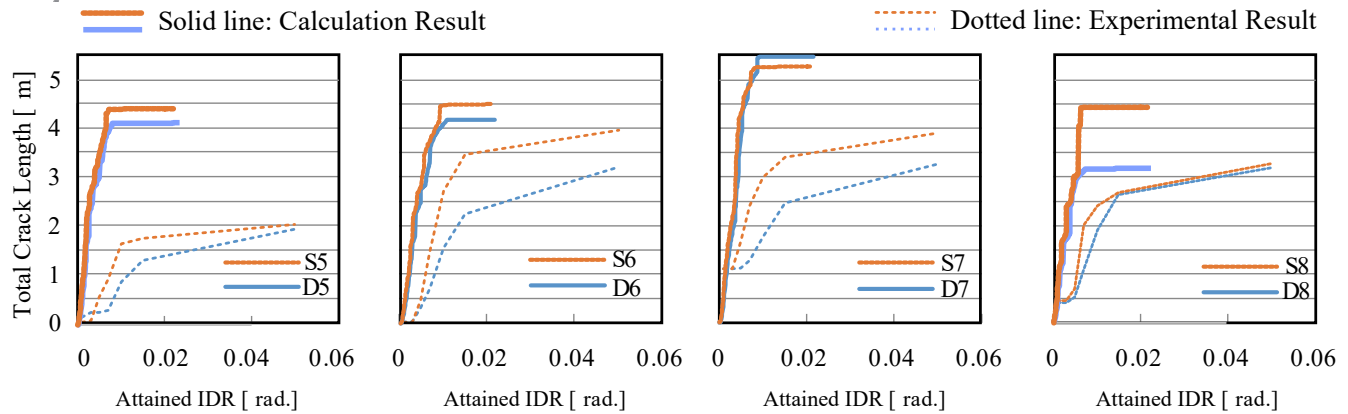


Fig. 16 – Comparison of crack length between the calculation results and experimental results

Table 5 shows the estimated cracking pattern after 7.5/1000 [rad.] and Fig.16 shows the comparison of crack length obtained from experimental results and analytical results. Observed crack length depends on the precision of image processing. The original video capture image has low-resolution and it could miss the extraction of small crack. Therefore estimated crack lengths of all specimen overestimate the experimental result. Additionally, the flexural-shear crack estimation would cause the overestimation of total crack length. Estimation results indicate that many flexural cracks occurred and they are grown to be a shear part of flexural-shear crack in Table 5, but experimental results indicate that a few flexural cracks occurred and they are not so grown to be a shear part of flexural-shear crack in Table 4. It implies that average flexural cracking space S_{av} [6] doesn't match with this case.

Although there is the tendency that the estimation crack length overestimates the experimental crack length, Fig. 16 indicates that the strain rate effects on the strength affect the estimation crack length as with experimental results. Specimen D5, D6, and D8 have the smaller crack length in the calculation results than that of specimen S5, S6, and S8, respectively. But specimen D7 has the larger crack length in the calculation results than that of specimen S7, and it doesn't follow the tendency of experimental result. Furthermore, an effect of the ratio of shear strength to flexural strength on the crack length difference between static loading and dynamic loading doesn't follow the tendency of experimental result. Specimens D5/S5 which have the ratio of shear strength to flexural strength around 1.8 and specimens D6/S6 which have the ratio of shear strength to flexural strength around 2.6 show the almost same difference in calculation results between static loading and dynamic loading. On the contrary, specimens D5/S5 and D8/S8 which have the ratio of shear strength to flexural strength around 1.8~1.9 show the quite difference in calculation results between static loading and dynamic loading. It is the future issues how to consider key factors like the ratio of shear strength to flexural strength, besides the strain rate effects on the strength, in the proposed simple method.

5. Conclusion

In this paper, very simple method of estimating the crack propagation under seismic load level with large deformation and under dynamic load were proposed and verified. The following finding were obtained.

- (1) Although there is the tendency of underestimating a shear crack length, some accuracy of the simple estimation method for crack length propagation under the static load with large deformation was shown.
- (2) The strain rate effect on the material strength affects slightly the estimation crack length as with experimental results. But an effect of the ratio of shear strength to flexural strength on the crack length difference between static loading and dynamic loading doesn't follow the tendency of experimental result. It is the future issues how to consider key factors like the ratio of shear strength to flexural strength in the proposed simple method.



6. References

- [1] Nagai, K., Sato, Y., Ueda, T. (2004): Mesoscopic simulation of failure of mortar and concrete by 2D RBSM, *Journal of Advanced Concrete Technology*, Vol.2, No.3, 359-374.
- [2] Belytschko T., Black T. (1999): Elastic crack growth in finite elements with minimal remeshing, *International Journal for Numerical Methods in Engineering*, Vol. 45, Issue 5, 601-620.
- [3] CEB-FIP (1978): Model Code for Concrete Structures
- [4] Kent D. C. and Park R. (1971): Flexural members with confined concrete, *Journal of Structural Division*, ASCE, Vol. 97, Issue 7, 1969-1990.
- [5] Okamura H., and Maekawa K. (1991): Nonlinear analysis and constitutive models of reinforced concrete, Gihodo Publishers (in Japanese)
- [6] Morita S. (1969): Allowable stress design of reinforcing bar due to the restricted concrete crack width, *Annual Report of Cement Technology*, Vol. 23, 552-556. (in Japanese)
- [7] Architectural Institute of Japan (2004): Guidelines for Performance Evaluation of Earthquake Resistant Reinforced Concrete Buildings (in Japanese)
- [8] Takahashi N. (2014): Simplified method of seismic damage prediction and visualization for R/C building structures, *Proc. of the Tenth U.S. National Conference on Earthquake Engineering*, Paper No.941.
- [9] Kaneko, T. (2002): Effect of strain rate on the load-restoring force characteristics of RC beam, University of Tokyo (in Japanese)